Antarctic Science 3 (3): 333–338 (1991)

Classification of Antarctic surfaces using AVHRR data: a multispectral approach

GIUSEPPE ZIBORDI and G. PAOLO MELONI

Institute for the Study of Geophysical and Environmental Methodologies, National Research Council, Via Emilia Est 770, 41100 Modena, Italy

Abstract: The mapping of sea, land ice, sea ice and clouds, from Advanced Very High Resolution Radiometer (AVHRR) images taken over Antarctica in daylight is investigated and a classification scheme is proposed on the basis of thresholds retrieved from multispectral patterns of representative data. The scheme, which can be used for real time analysis of AVHRR images in scientific and logistic activities, gives satisfactory separation of different categories. Major misclassification occurs between ice clouds and land ice because of their very similar spectral signature in the AVHRR channels. Comparison of classified samples, obtained from visual inspection of images and from application of the scheme, exhibits a confusion matrix with accuracy A=92% over areas almost free from ice clouds.

Received 7 September 1990, accepted 5 May 1991

Key words: Advanced Very High Resolution Radiometer, clouds, land ice, remote sensing, sea ice

Introduction

Satellites, giving synoptic information of the earth's surface, are a useful aid in atmospheric physics (Kergomard & Tanrè 1989), oceanography (Sullivan *et al.* 1988, Schluessel & Grassl 1990), glaciology (Gloersen & Campbell 1988; Hall *et al.* 1989), and meteorology (Key *et al.* 1989) in Antarctica because of the difficulty in exploring its extensive, remote and inhospitable territory.

The Advanced Very High Resolution Radiometer (AVHRR), installed on NOAA's satellites, has great importance in operational and research activities because of the high frequency of revisiting the same area and capability of obtaining measurements of the earth's surface with 1.1 km resolution (at nadir) in five spectral bands (Lauritson *et al.* 1979). These are the red (channel 1: 0.58–0.68 μm), near infrared (channel 2: 0.72–1.10 μm), middle infrared (channel 3: 3.55–3.93 μm) and thermal infrared (channel 4: 10.3–11.3 μm and, only on board NOAA-odd satellites, channel 5: 11.5–12.5 μm) spectral bands. The use of AVHRR data in scientific and logistic activities related to Antarctic regions requires the discrimination of different categories such as sea, snow, ice and clouds in the image.

Schemes proposed for surface and cloud classification from AVHRR data taken over medium latitude regions (Inoue 1987, Saunders & Kriebel 1988), are not optimized for polar regions where emittance and reflectance similarity for clouds, snow and ice are the main source of misclassification. Schemes proposed for polar regions (Ebert 1987, Key *et al.* 1989, Welch *et al.* 1990) do not satisfy requirements of low computing time needed for real-time use of data.

A scheme is proposed, based on the threshold technique with identification of patterns for each category in the multidimensional radiance space formed by multispectral data taken over training areas. This has been set up to support real-time image analysis during summertime Antarctic expeditions. The purpose of this paper is the description of the classification scheme.

Classification methodology

The classification scheme has been mainly set up to produce sea ice maps and provide masking for sea surface temperature (SST) maps. Because of the real-time use of data in supporting navigation (by sea ice maps) and oceanographic campaigns (by SST maps), the required low computing time has been obtained by adopting a fast classifier and by selecting few categories representative of the Antarctic surface.

Categories

The following categories are distinguished:

a) open sea
b) land ice (in this paper this category is taken to include ice shelves and land areas covered by snow and ice)
c) sea ice (in this paper this category is taken to include pack, floes and bergs)
d) clouds (including thin clouds, water clouds and ice clouds).

Land free of snow and ice is not accounted for in the classification scheme, because of the difficulty in distinguishing between land and shadowed surfaces that, added to the relative low resolution of AVHRR (the sensor

footprint generally is larger than land areas free of snow and ice), make it almost impossible to create a training set of data for this category.

Data reduction

The study of patterns for each category has been performed using AVHRR images, taken over Victoria Land and the Ross Sea in the period January–February 1990. Training sets to create multispectral patterns have been obtained from radiance measured in channels 1, 2, 3 and 4 over representative areas (channel 5 has not been used in order to maintain compatibility of the classification scheme with NOAA-even and NOAA-odd satellite data). Radiance has been computed from digital number DN_n, for each channel n, by using the linear relationship

$$Ln = a_n + b_n DN_n$$

where the constants a_n and b_n, for channels 1 and 2, have been obtained from pre-flight values according to the method given by Price (1988) while, for channels 3 and 4, they have been taken from ancillary data of images. The constants a_n and b_n are given in Table I.

Degradation of sensivity in channels 1 and 2, which could be as high as several percent each year (Teillet *et al.* 1990) and which is not accounted for in constants a_n and b_n (because of their evaluation from pre-flight values), is a perturbing factor in the use of absolute thresholds for multitemporal data analysis. In this study, since the used images have been taken during a relatively short period (less than two months), the change of sensor sensivity in channels 1 and 2 has been assumed to have negligible effect in the classification of data.

Radiance, measured by AVHRR in different regions of the electromagnetic spectrum, results from different radiative processes: in channels 1 and 2 it is due to solar radiance reflected by the earth's surface and clouds into the sensor field of view; in channel 3 it is the sum of contributions due to solar reflected and terrestrial emitted radiance; in channel 4 it is due only to terrestrial emitted radiance. To avoid dependence of data on geometrical illumination of the earth, radiance measured in channels 1 and 2 has been normalized with respect to the sun zenith and sun-earth distance, through the relationship

$$\langle L \rangle_i = L_i \, d/\mu$$

where i=1,2, d is a parameter accounting for the sun-earth distance (Jackson and Slater 1986) and μ is the cosine of the sun zenith angle.

Table I. Calibration constants used fro AVHRR (NOAA-11) data.

Channel	1	2	3	4
	$\left(\frac{W}{m^2 \mu m\ sr}\right)$	$\left(\frac{W}{m^2 \mu m\ sr}\right)$	$\left(\frac{nW}{m^2 \mu m\ sr}\right)$	$\left(\frac{\mu W}{m^2 \mu m\ sr}\right)$
a_n	-19.37	-11.38	146.29*	16.9988*
b_n	0.4705	0.2775	-0.148*	-0.01712*

* from ancillary data of orbit 6753

Analysis of multispectral patterns

Training sets of radiance data have been taken from full resolution images by visual selection of elements representative of the different categories to be interpreted. Radiance retrieved from images detected with sun zenith between 60 and 70 degrees (orbits: 6682, 6753, 6879, 6936, 7063), have been used to produce scatter plots given in Fig. 1. Data obtained from channel 2 have been used because of their lower dependence on atmospheric scattering than data from channel 1 (scattering decreases contrast among different surfaces).

Cloud type may be shown on scatter plots using known radiative properties of clouds. Water clouds are mainly characterized by high reflectivity in channel 3 of AVHRR (Kidder & Wu 1984). In fact, due to the high value of the water refractive index at around 3 μm, the sun radiance is reflected by clouds and increases as the cloud layer optical thickness increases and as the size of water droplets decreases (Hunt 1973, Arking & Childs 1985). Because of this feature (see Fig. 1a), discrimination of relatively warm water clouds can be carried out by applying a threshold to radiance in channel 3 (normalization of the reflected radiance contribution in channel 3 is avoided by applying a threshold that is not critical even with different daylight illumination conditions).

Thin clouds, characterized by a low optical thickness, exhibit low reflectivity in the visible and near infrared. Detection of these clouds over land ice is quite difficult because of their negligible effect on the radiance field of the underlying surface. In contrast over the sea, thin clouds can be discriminated from the contiguous classes such as open sea and sea ice, because of the lower radiance in channel 4 (see Fig. 1b).

Clouds characterized by high percentage of ice crystals in the upper layer, here referred as to ice clouds, have a spectral signature very similar to land ice: low brightness temperature in the thermal infrared, high reflectivity in the visible and poor reflectivity (Hunt 1973, Scorer 1989) in the middle infrared due to ice-crystal absorption. It may be possible to discriminate between ice clouds and land ice by using the ratio between radiance in channel 2 and in channel 1 (or the difference between the normalized radiances in channels 1 and 2).

In fact, theoretical computations (Dozier 1989) show:

a) decrease from red toward near infrared, as a function of the radii of grains, in the snow reflectance and
b) an almost constant value, depending on the radii of water droplets and of ice crystals, in the reflectance of water clouds and ice clouds respectively.

This would suggest the possibility of obtaining separate patterns for clouds and land ice by plotting the ratio between the radiances in channels 2 and 1 (or the difference between

the normalized radiances in channels 1 and 2), against the radiance in channel 3. However this ratio, like the difference, computed with actual radiances, produces scattered cloud data overlapping with the land ice pattern (see Fig. 1c) and thus it does not completely fulfil requirements for ice cloud mapping.

From analysis of scatter plots some general conclusions can be drawn:

a) the open sea category is defined by a pattern having no overlapping area with other patterns, making its discrimination from other categories accurate (see Fig. 1b)
b) accurate separability of ice clouds and land ice cannot be obtained because of their very similar spectral signature in the AVHRR channels and
c) normalization of radiance in channel 2 is required to reduce the indeterminacy caused by different illumination conditions in separating contiguous (i.e. open sea and sea ice) or overlapping (i.e. sea ice and land ice) categories by thresholds (normalization of the radiance has been seen to be unreliable at sun zenith larger than about 75 °).

Misclassification of elements pertaining to contiguous or overlapping categories could be produced by perturbing effects such as:

a) increase of view angle which causes an increase in the detected radiance due to an increase in optical path through atmosphere (the resulting radiometric aberration makes the classification of data at the edge of image very difficult);
b) specular reflection of direct sun radiance (sun glint) by sea, snow and ice surfaces that gives very high radiance values (this effect is mainly restricted to the edge of image because of the low sun elevations in polar regions).

These perturbing effects have not been corrected because of difficulty in performing accurate modelling of atmospheric and surface reflected radiance at view angles higher than about 50° (Tanrè *et al.* 1986) where aberration becomes very high. The ratio between radiance in channel 2 and in channel 1, instead of the simple normalized radiance in channel 2, could contribute to the reduction of view angle effects. However, use of the ratio between radiance in the two channels strongly reduces the ability to discriminate between land ice and sea ice as shown in Fig. 1c.

The classifier

The classifier separates categories according to decision regions defined by radiance limits evaluated from scatter plots of training sets given in Fig. 1. The scheme develops by evaluating the relevance of each image element to subsequent regions (w_{1a}, w_{1b}, w_{1c}, w_2, w_3) and it stops when the element is found to belong to one region. Elements which do not pertain to any of the defined decision regions are filled as land ice. Such a classification is very fast but, as a drawback, has a low ability in discriminating correlations

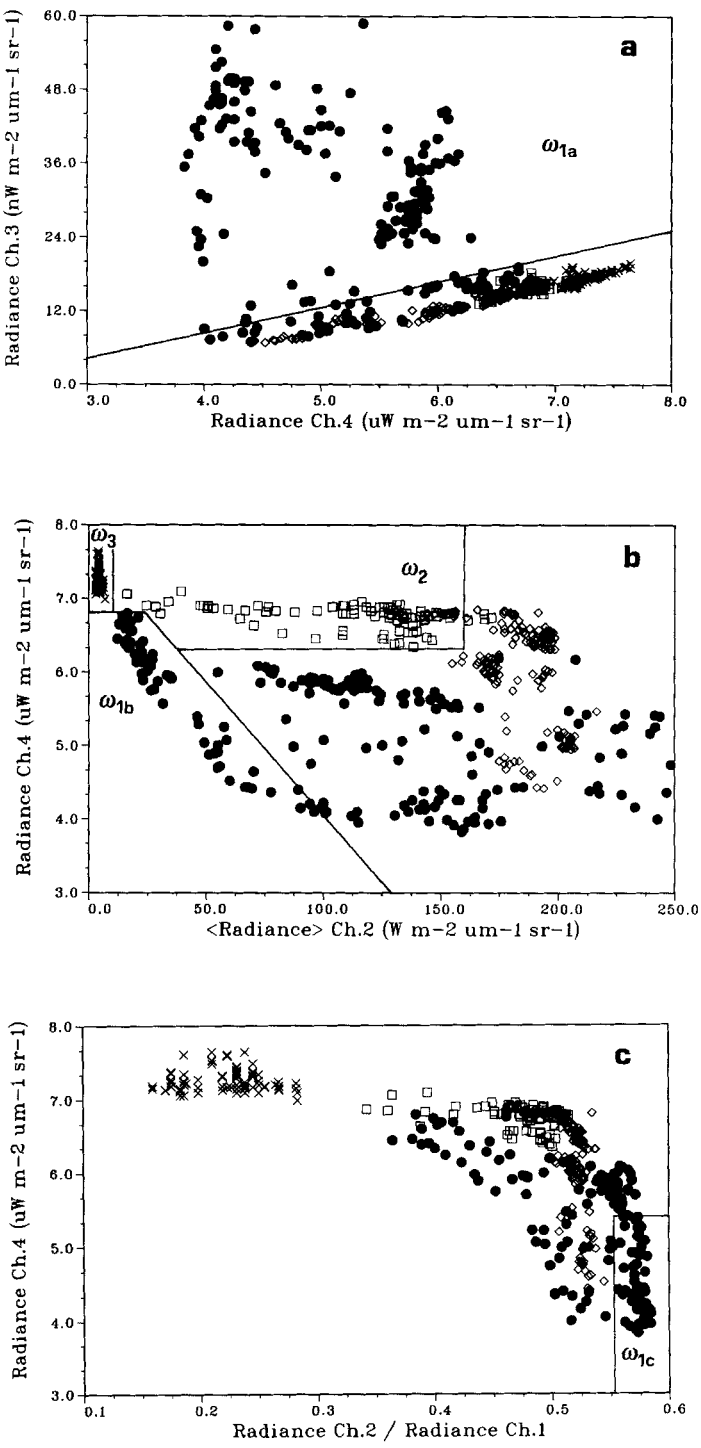

Fig. 1. Scatter plots of: **a.** radiance in channel 4 against radiance in channel 3; **b.** normalized radiance (i.e. <Radiance>) in channel 2 against radiance in channel 4; **c.** ratio of radiance in channel 2 to radiance in channel 1, against. radiance in channel 4 (open sea (x); sea ice (□); land ice (◇); clouds (●)). Straight lines specify the decision regions used in the classification scheme for the different categories (w_{1a}: water clouds; w_{1b} thin clouds; w_{1c} ice clouds; w_2 sea ice; w_3 open sea).

between overlapping decision regions (Lillesand & Monsour 1979).

Sea ice coverage

The average radiance measured over the sensor footprint in the presence of water (leads, polynyas) with very low reflectance and ice (floes, bergs) generally covered by snow with very high reflectance, can be related to sea ice coverage. The percentage coverage of sea ice C, assumed to have a linear dependence on radiance in the near infrared (Comiso & Zwally 1982), can be computed, for each element of the category, using the relationship:

$$C = \frac{<L>_2 - <L_W>_2}{<L_I>_2 - <L_W>_2} \times 100$$

where $<L>_2$ is the input radiance in channel 2, and $<L_W>_2$ and $<L_I>_2$ are the highest open sea radiance and the lowest land ice radiance thresholds (evaluated from scatter plot in Fig. 1b), ideally corresponding to 0% and 100% ice cover respectively. The method used for the evaluation of sea ice cover is likely to give underestimated values in presence of cloud shadowing of the surface.

Results and discussion

The developed multispectral classification scheme has been tested with several images taken in January–February 1990 over Victoria Land and Ross Sea in East Antarctica. To have an estimate of the actual classification accuracy outside areas affected by ice clouds, the scheme has been checked with sample data independent of those used for pattern construction (even if taken from the same images). Elements of sub-images not significantly affected by ice clouds have been visually classified and compared with output data of the scheme. The confusion matrix (Estes *et al.*1983) given in Table II, obtained with 500 radiance samples, exhibits an accuracy close to A=92%. A decrease in accuracy is expected as the percentage of ice clouds increases.

Analysis of results has shown that minor misclassification, besides that between ice clouds and land ice, occurs with sub-categories characterized by very similar spectral signature in the AVHRR channels. Examples of such misclassification are:

a) glacier ice which could be classified as sea ice
b) land ice on shadowed surfaces or on orientated surfaces reflecting direct sun radiance, which could be classified as cloud
c) thin clouds over land ice classified as land ice
d) land areas free of snow and ice classified as cloud or land ice
e) floes or bergs several times larger than the sensor footprint, that could be classified as land ice.

Pictures obtained from AVHRR data, converted to radiance units with added coastline and latitude-longitude grids (using SHARK facilities (Pittella & Bamford 1989)), are given in Fig. 2. The pictures highlight the very low capability of single channel data to separate different categories. The classified image and the geographical area, corresponding to data of Fig. 2, are shown in Fig. 3. The percent of radiances in each category, obtained from the classification of the image in Fig. 2,is shown in Table III.

Results of a similar analysis obtained from several images are given in Table IV. Data have been computed by averaging percentages obtained from classification of nine sub-images of 512x512 elements, taken approximately over the same area centred at about 166°E and 75° 30'S and related to orbits: 6682, 6753, 6865, 6879, 6893, 6907, 6922, 6936, 7063. It must be noted that for these examples, which were almost free from ice clouds, approximately 97% of cloud filled radiances are singled out as water clouds.

The percentage of sea ice obtained from AVHRR data has been compared with visual observation carried out by ships and helicopters at approximately the same time. Differences between the two methods were less that 15% within the investigated area.

Conclusions

Table II. Confusion matrix of sample AVHRR data

Known category*	Number of elements	% correct	No. of elements classified in categ. 1	2	3	4
1	128	94%	120	4	0	4
2	87	83%	0	72	0	15
3	80	100%	0	0	80	0
4	205	90%	8	12	0	185

*1: clouds; 2: sea ice; 3: open sea; 4: land ice

Table III. Percentage of elements in image shown in Fig. 2 belonging to the different decision regions.

	w_{1a}	w_{1b}	w_{1c}	w_2	w_3	-
Category*	1	1	1	2	3	4
Percentage	25.5	0.3	0.1	34.1	3.8	36.2

* 1: clouds; 2: sea ice; 3: sea; 4: land ice

Table IV. Percentage of elements from nine images taken over the same area in different days, belonging to the different decision regions (the standard deviation is given in braces).

	w_{1a}	w_{1b}	w_{1c}	w_2	w_3	-
Category*	1	1	1	2	3	4
Percentage	37 (14.1)	0.8 (1.0)	0.3 (0.3)	32.3 (6.9)	5.6 (2.1)	24.0 (8.8)

*1: clouds; 2: sea ice; 3: sea; 4: land ice

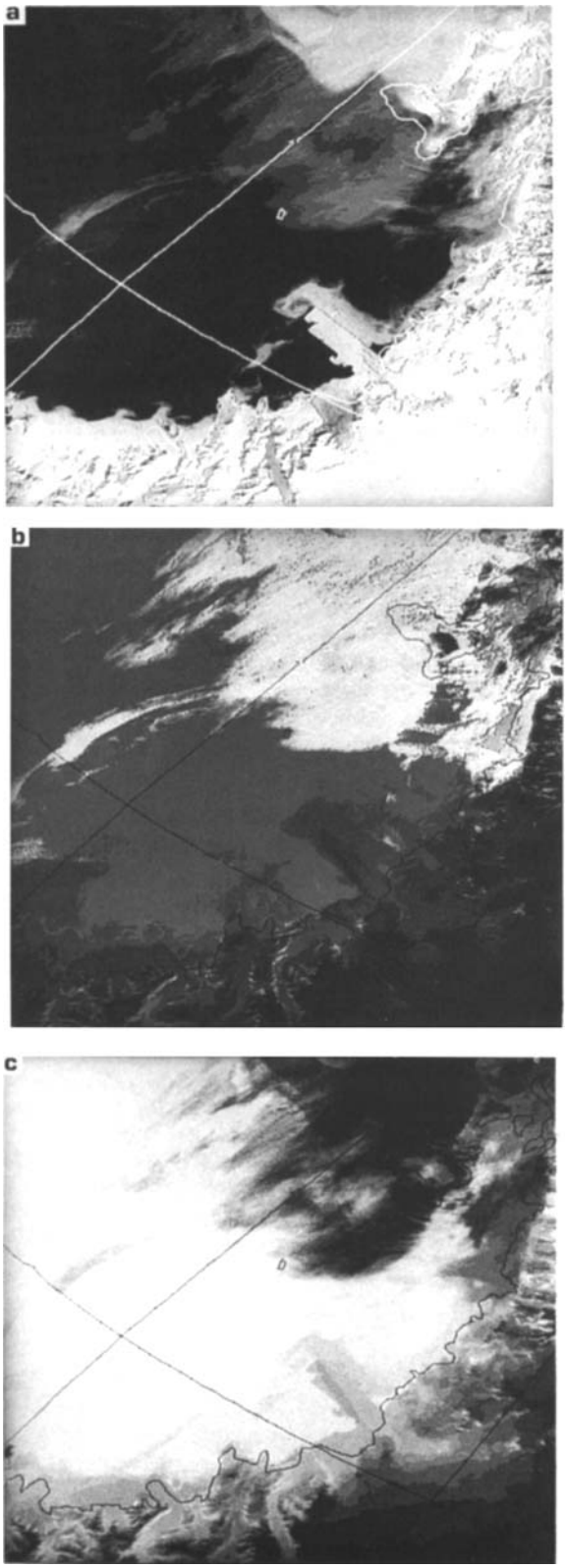

Fig. 2. Images obtained from NOAA-11 data (sub-images of 512 x 512 elements) displaying Victoria Land and Ross Sea, centred at about 166° E and 75°30'S, taken on 7 February 1990, orbit 7063: **a.** channel 2, **b.** channel 3, **c.** channel 4. In this figure an increase in brightness indicates an increase in radiance.

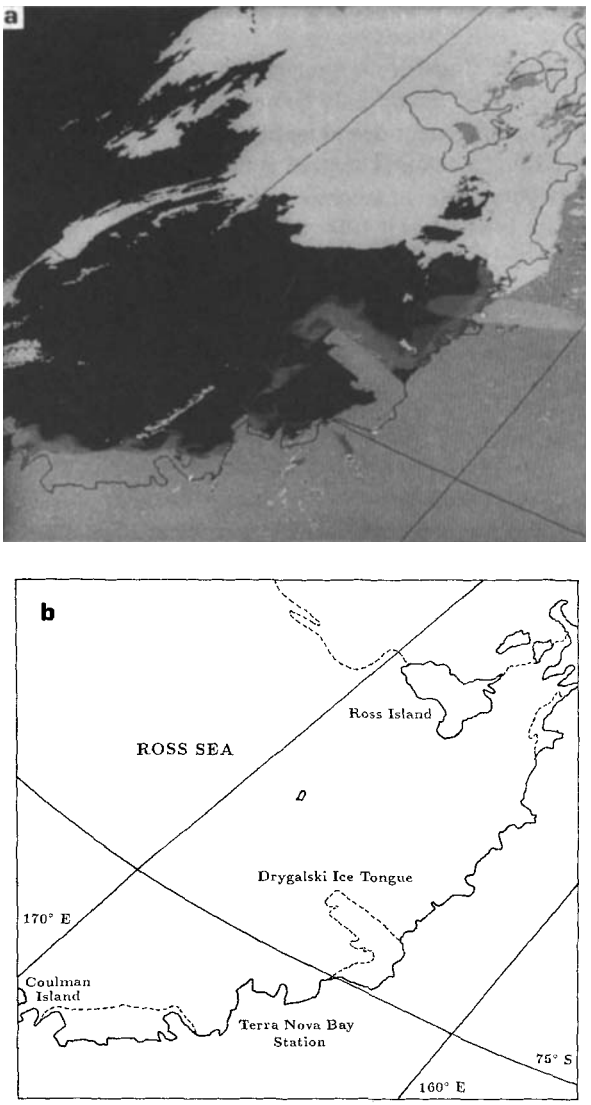

Fig. 3. a. The classified map constructed from the AVHRR of Fig. 2. Clouds are white, open sea is black, land ice is light grey and sea ice is dark grey. In the sea ice category, increasing brightness indicates an increase percentage sea ice cover. **b.** The geographical area covered by analysis.

Satisfactory results have been obtained in the mapping of sea ice, open sea, land ice and clouds from several daylight images taken over Victoria Land and the Ross Sea with different illumination conditions. Comparison of classified examples, retrieved from visual inspection of AVHRR images and obtained by applying the threshold scheme, has given a confusion matrix with accuracy close to 92% over areas not significantly affected by ice clouds. The major limitation of the proposed multispectral classification scheme lies in the discrimination of ice clouds from land ice, because of their very similar spectral signature in the AVHRR channels.

An improvement of the scheme may be possible by introducing textural analysis (Liljas 1989, Welch *et al.* 1990). In fact, a better separability between ice clouds and

land ice is expected to be achieved because of the feathery appearance of ice clouds as opposed to the more homogenous snow surface. Further improvement of the classification of Antarctic covers would only be possible if further spectral information on categories to be interpreted were available. For example, a channel centred at about 1.6 μm or 2.2 μm could be very useful in separating clouds and snow (Crane & Anderson 1984, Dozier 1989, Masuda & Takashima 1990).

Acknowledgements

This work was supported by the Italian National Antarctic Research Program. The authors wish to acknowledge G.Pittella, C.Bamford and A.Buongiorno of the European Space Agency for their help with the image analysis.

References

ARKING, A. & CHILDS, J.F. 1985. Retrieval of cloud cover parameters from multispectral satellite images. *Journal of Climate and Applied Meteorology*, **24**, 322-333.

COMISO, J.C. & ZWALLY, H.I. 1982. Antarctic sea ice concentration inferred from Nimbus 5 ESMR and Landsat Imagery. *Journal of Geophysical Research*, **87**, 5836-5844.

CRANE, R.G. & ANDERSON, M.R. 1984. Satellite discrimination of snow/cloud surfaces. *International Journal of Remote Sensing*, **5**, 213-223.

DOZIER, J. 1989. Spectral signature of alpine snow cover from Landsat Thematic Mapper. *Remote Sensing of Environment*, **28**, 9-22.

EBERT, E. 1987. A pattern recognition technique for distinguishing surface and cloud types in the polar regions. *Journal of Climate and Applied Meteorology*, **26**, 1412-1427.

ESTES, J.E. HAJIC, E.J. & TINNEY, L.R. 1983. Fundamentals of image analysis of visible and thermal infrared data. *In* SOMONETT, D.S. *ed. Manual of Remote Sensing, Second Edition, Volume 1.* Falls Church: American Society of Photogrammetry, 987-1124 (1232pp).

GLOERSEN, P. & CAMPBELL, W.J. 1988. Variations of the Arctic, Antarctic, and global sea ice covers during 1978-1987 as observed with the Nimbus 7 Scanning Multichannel Microwave Radiometer. *Journal of Geophysical Research*, **93**, 10666-10674.

HALL, D.K., CHANG, A.T.C., FOSTER, J.L., BENSON, C.S. & KOVALICK, W.M. 1989. Comparison of it *in situ* and Landsat Derived Reflectance of Alaskan Glaciers. *Remote Sensing of Environment*, **28**, 23-21.

HUNT, G.E. 1973. Radiative properties of terrestrial clouds at visible and infra-red thermal window wavelengths. *Quarterly Journal of the Royal Meteorology Society*, **99**, 346-369.

INOUE, T. 1987, A cloud type classification with NOAA 7 Split-Window measurements. *Journal of Geophysical Research*, **92**, 3991-4000.

JACKSON, R.D. & SLATER P.N. 1986. Absolute calibration of field reflectance radiometers. *Photogrammetric Engineering and Remote Sensing*, **52**, 189-196.

KIDDER, S.Q. & WU, H. 1984. Dramatic contrast between low clouds and snow cover in daytime 3.7 μm imagery. *Monthly Weather Review*, **112**, 2345-2346.

KERGOMARD, C. & TANRÈ, D. 1989. On the satellite retrieval of aerosol optical thickness over polar regions. *Geophysical Research Letters*, **16**, 707-710.

KEY, J.R., MASLANIK, J.A. & BARRY, R.G. 1989. Cloud classification from satellite data using a fuzzy sets algorithm: a polar example. *International Journal of Remote Sensing*, **10**, 1823-1842.

LAURITSON, L., NELSON, G.J. & PORTO, F.W. 1979. Data extraction and calibration of TIROS-N/NOAA radiometers. *NOAA technical memorandum* NESS 107, 58pp.

LILJAS, E. 1989. Experience on an operational cloud classification method. *In* BRIDGE, G. *ed. Proceedings of the 4th AVHRR data users meeting*, Darmstadt-Eberstadt: EUMETSAT, 73-78 (349pp).

LILLESAND, T.M. & MONSOUR, E.M. 1979. *Remote sensing and image interpretation.* New York: John Wiley and Sons, 721 pp.

MASUDA, K. & TAKASHIMA, T. 1990. Deriving cirrus information using the visible and near-IR channels of the future NOAA-AVHRR radiometer. *Remote Sensing of Environment*, **31**, 65-81.

PITTELLA, G. & BAMFORD, C. 1989. The Earthnet "SHARK" system for TIROS data acquisition processing and archive. *In* BRIDGE, G. *eds. Proceedings of the 4th AVHRR data users meeting*, Darmstadt-Eberstadt: EUMETSAT, 73-78 (349pp).

PRICE, J.C. 1988. An update on visible and near infrared calibration of satellite instruments. *Remote Sensing of Environment*, **24**, 419-422.

SAUNDERS, R.W. & KRIEBEL, K.T. 1988. An improved method for detecting clear sky and cloudy radiances from AVHRR data. *International Journal of Remote Sensing*, **9**, 123-150.

SCHLUESSEL, P. & GRASSL, H. 1990. SST in polynyas: a case study. *International Journal of Remote Sensing*, **11**, 933-945.

SCORER, R.S. 1989. Cloud reflectance variations in channel-3. *International Journal of Remote Sensing*, **10**, 675-686.

SULLIVAN, C.W., MCCLAIN, C.R., COMISO, J.C. & SMITH, W.O. 1988. Phytoplankton standing crops within an Antarctic ice edge assessed by satellite remote sensing. *Journal of Geophysical Research*, **93**, 12487-12498.

TANRÈ, D., DEROO, C.M., DUHAUT, P., HERMAN, M., MORCRETTE J.J., PERBOS, J. & DESCHAMPS, P.Y. 1986. Simulation of the Satellite Signal in the Solar Spectrum (5S): Users Guide. Villeneuve D'Ascq, France: Laboratoire d'Optique Atmospherique, Université de Lille, 150pp.

TEILLET, P.M., SLATER, P.N., DING, Y., SANTER, R.P., JACKSON, R.D. & MORAN, M.S. 1990. Three methods for the absolute calibration of the NOAA AVHRR sensor in-flight. *Remote Sensing of Environment*, **31**, 105-120.

WELCH, R.M., KUO, K.S. & SENGUPTA, S.K. 1990. Cloud and surface features in polar regions. *IEEE Transaction on Geoscience and Remote Sensing*, **28**, 520-528.